

## Measurement of Radiative Pion-Proton Scattering near the $\Delta(1236)$ Resonance\*

M. Arman, D. J. Blasberg, R. P. Haddock, K. C. Leung, B. M. K. Nefkens,  
B. L. Schrock, D. I. Sober, and J. M. Sperinde

*Department of Physics, University of California, Los Angeles, California 90024*

(Received 10 July 1972)

We have measured the differential cross section for radiative  $\pi^+$ -proton scattering,  $\pi^+p \rightarrow \pi^+p\gamma$ , at 294 MeV under kinematical conditions favorable to the observation of radiation from the magnetic dipole moment of the  $\Delta^{++}(1236)$  resonance. For radiated photon energies above 30 MeV, our data do not agree with explicit theoretical calculations which include an estimate of the magnetic moment radiation. Rather, our data agree with the simple expression in the c.m. system,  $d\sigma/d\tilde{\Omega}_\pi d\tilde{\Omega}_\gamma d\tilde{E}_\gamma = \sigma_0/\tilde{E}_\gamma$ , over the full range of photon energy, up to  $\tilde{E}_\gamma = 140$  MeV. Preliminary measurements of radiative  $\pi^-$ -proton scattering have also been made.

Radiative pion-proton scattering,

$$\pi^+p \rightarrow \pi^+p\gamma, \quad (1)$$

has been the object of many theoretical investigations,<sup>1-8</sup> although its experimental observation up to the present has been limited to 26 events.<sup>9,10</sup> It has been suggested<sup>1-3</sup> that a measurement of Reaction (1) can be used to determine  $\mu(\Delta^{++})$ , the magnetic dipole moment of the  $\Delta^{++}(1236)$   $\pi$ - $N$  resonance. This novel procedure<sup>11</sup> for determining a magnetic moment is based on the process depicted in the Feynman diagram of Fig. 1. The width of the  $\Delta^{++}$  allows it to emit a photon and remain with its quantum numbers unchanged. In this process the radiation due to the magnetic dipole moment dominates over the radiation due to the quadrupole moment.<sup>3</sup> There is an explicit prediction for  $\mu(\Delta^{++})$  given by SU(6), namely,<sup>12</sup>  $\mu(\Delta^{++}) = 2\mu(p)$ , where  $\mu(p)$  is the magnetic dipole moment of the proton.

Radiative scattering is ordinarily dominated by external bremsstrahlung, in which a photon is emitted by an incoming or outgoing charged particle. When the colliding particles have the same charge, the amplitudes for radiation by the incoming and outgoing pion and proton interfere destructively. Under the correct kinematical conditions, this interference can result in a suffi-

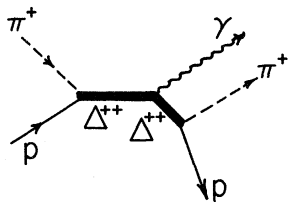


FIG. 1. Feynman diagram for magnetic-dipole-moment contribution to radiative  $\pi^+p$  scattering.

ciently reduced emission of external bremsstrahlung so that effects of internal structure, such as the process of Fig. 1, can be observed. The external bremsstrahlung is smallest when the photon is emitted backward and at large angles to both the scattered pion and proton directions. In such a configuration, the photon spectrum above 20 MeV in the laboratory, for 300-MeV incident  $\pi^+$ , is predicted<sup>1-3</sup> to depend sensitively on the magnetic dipole moment of the  $\Delta^{++}$ . The expected cross section is small,  $d\sigma/d\Omega_\pi d\Omega_\gamma dE_\gamma \approx 10^{-3} \mu\text{b}/\text{sr}^2 \text{ MeV}$ , which necessitates the use of detectors with a large solid angle.

We report here a measurement of radiative pion-proton scattering in a geometry sensitive to the magnetic-moment radiation of the  $\Delta^{++}(1236)$ . The experiment was carried out at the Lawrence Berkeley Laboratory 184-in. cyclotron with the apparatus shown in Fig. 2. The energy of the incident beam was  $294 \pm 4$  MeV with  $\Delta p/p = \pm 2.6\%$  and the rate was about  $1.5 \times 10^6 \pi^+/\text{sec}$ . The beam was defined by two counter hodoscope planes  $V$  and  $H$  and by a small counter  $T$  (see Fig. 2). Events with multiple pions in the same beam bunch were suppressed by means of anti counters and rejection of double counts in the hodoscope. The hydrogen target consisted of a flat Mylar flask, 5 cm wide and filled with liquid hydrogen, which was surrounded by a second Mylar flask that acted as a gas ballast. These flasks were inside a 0.7-mm aluminum can. The target axis made an angle of  $20^\circ$  with respect to the beam, to minimize the scattering of the outgoing protons. The scattered pions were detected in a spectrometer consisting of three  $1 \times 1$ -m wire spark chambers, a  $180 \times 45$ -cm magnet with a 45-cm gap mounted to deflect particles vertically, three more wire spark chambers, and four contiguous counters. With this setup, we could de-

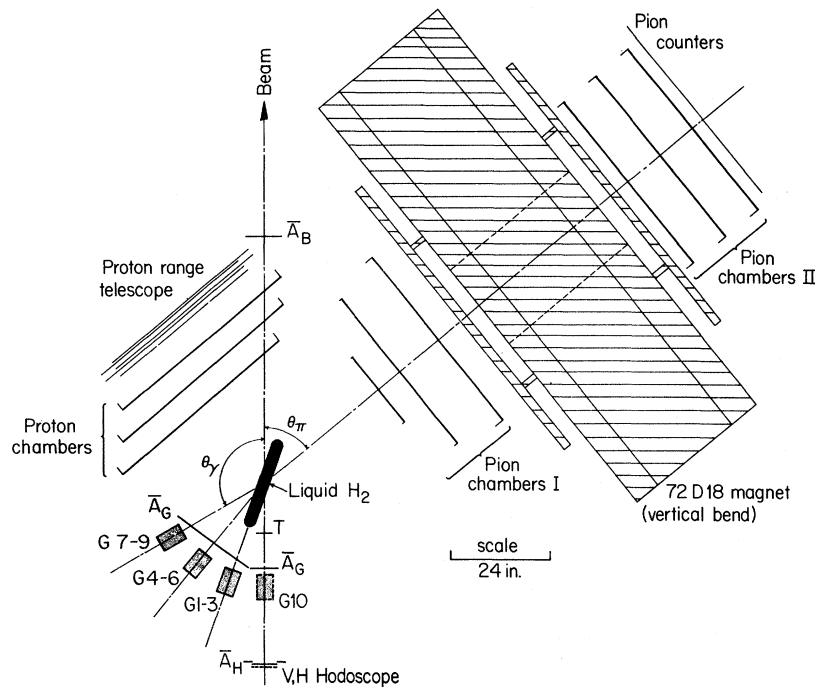


FIG. 2. Experimental apparatus. Photon counter G10 is positioned below the beam line.

termine the scattered pion momentum to  $\pm 1\%$ . The acceptance of the pion detected was  $-43.5^\circ > \theta_\pi > -56.5^\circ$  and  $-10^\circ < \varphi_\pi < 22^\circ$ , where  $\theta$  is measured from the beam line in the horizontal plane and  $\varphi$  is measured from the horizontal plane. The recoil protons were detected by three  $1 \times 1$ -m wire spark chambers and a six-plane range telescope. The proton energy resolution of this system was about  $\pm 8$  MeV. The acceptance of the proton detector was  $10^\circ < \theta_p < 63^\circ$  and  $-26^\circ < \varphi_p < +26^\circ$ . The photons were detected in ten lead-glass Cherenkov counters, each  $10 \times 10$  cm in area and 15 cm thick, or about 5.2 radiation lengths. The efficiency of these counters was determined indirectly<sup>13</sup> from measurements of their efficiency for electrons of energies between 9 and 25 MeV. The counters were  $(98 \pm 2)\%$  efficient for electrons of 16 MeV and above. The photon efficiency for a given incident-photon path was calculated by a Monte Carlo procedure using the measured electron efficiency as input and considering pair production and Compton scattering to be the interaction processes. The efficiency for a normally incident photon was found to be  $(81 \pm 5)\%$  at  $E_\gamma = 20$  MeV and  $(92 \pm 2)\%$  at  $E_\gamma = 50$  MeV. The location of the ten counters was between  $180^\circ > \theta_\gamma > 120^\circ$  and  $-36^\circ < \varphi_\gamma < 0^\circ$  (see Fig. 2). The photon counters were covered by large anti counters. An on-line PDP-8 computer re-

corded all relevant data for each event: the information from the nine wire spark chambers, all counters, and the proton, pion, and photon times of flight. These data were transformed off-line into kinematical quantities.

Our analysis program made a two-constraint fit of every analyzable event to the hypothesis  $\pi^+p \rightarrow \pi^+p\gamma$ , using our measured value for the incident and scattered pion energy and direction and also the angles of the recoil proton and photon. Three cuts were applied to the data. First, we removed all events that had a reconstructed  $E_\gamma < 10$  MeV. This cut eliminated elastic-scattering events in coincidence with a random trigger in a photon counter. This was our major background, since elastic-scattering events satisfy the radiative-scattering hypothesis with  $E_\gamma = 0$ . Second, we applied a time-of-flight cut on the photon counters of  $\pm 3$  nsec. The event trigger had accepted photons within a  $\pm 13$ -nsec window. The time-of-flight distribution showed that the majority of events with reconstructed photon energies below 10 MeV were indeed due to a random trigger in a photon counter. Third, we applied a cut on the reconstructed missing mass of the neutral particle to remove all events of the type  $\pi^+p \rightarrow \pi^+p\pi^0$ , which formed a clearly distinguishable peak separate from the radiative events. The pseudo  $\chi^2$  distribution of our remain-

ing events consisted of a large peak of 647 true  $\pi^+p \rightarrow \pi^+p\gamma$  events and a very small background, less than 3%. Empty-target data were analyzed, and yielded so few acceptable events that no subtraction was necessary. Further details of the analysis are given by Arman.<sup>14</sup>

We have also calculated from our data the differential cross sections for  $\pi^\pm p \rightarrow \pi^\pm p$  and the total cross section for  $\pi^\pm p \rightarrow \pi^\pm p\pi^0$ . The elastic-scattering measurement provides a test of the acceptance and efficiency of the proton- and pion-detection system and the data analysis, whereas the  $\pi^0$  production tests the performance of the entire system at kinematic conditions resembling those of high-energy photon emission. The results at  $T_\pi = 294$  MeV and  $\theta = 68^\circ$  are  $d\sigma(\pi^+p \rightarrow \pi^+p)/d\hat{\Omega} = 6.2 \pm 0.5$  mb/sr and  $d\sigma(\pi^+p \rightarrow \pi^+p\pi^0)/d\hat{\Omega} = 0.90 \pm 0.06$  mb/sr, which agree with the values of  $5.7 \pm 0.3$  and  $0.92 \pm 0.04$  mb/sr from the CERN phase-shift solutions.<sup>15</sup> (The tilde denotes center-of-mass variables.) For  $\pi^0$  production, we assume the angular distribution of the  $\pi^0$  to be isotropic in the center of mass, and obtain  $\sigma_i(\pi^+p \rightarrow \pi^+p\pi^0) = 0.12 \pm 0.05$  mb, which is in good agreement with the published value<sup>9</sup> of  $0.11 \pm 0.04$  mb. For the ratio of the differential cross section for  $\pi^0$  production by  $\pi^+$  and  $\pi^-$ , we find  $d\sigma(\pi^-p \rightarrow \pi^-p\pi^0)/d\sigma(\pi^+p \rightarrow \pi^+p\pi^0) = 0.96 \pm 0.10$ , which agrees with the published<sup>9, 10, 16</sup> ratio of  $0.85 \pm 0.40$  for the total cross sections.

Our measured  $\pi^+p \rightarrow \pi^+p\gamma$  cross section in the laboratory frame, differential in the photon energy and in the angles of the scattered pion and photon, for our choice of geometry, is shown in Fig. 3(a). We also show the published predictions<sup>1, 2, 17</sup> recalculated for our geometry, for different values of  $\mu(\Delta^{++})$ . The manifestation of the magnetic dipole moment of the  $\Delta^{++}$  as predicted by these calculations is not seen in our data. The curve labeled "soft photon approximation" was calculated from the first two terms of the gauge-invariant expansion of the radiative amplitude developed by Low.<sup>17</sup> Fischer and Minkowski<sup>1</sup> have generalized this approach to resonant scattering and have shown how to add the radiation of the  $\Delta(1236)$ . Reference 2 uses an effective Lagrangian which includes interactions between meson, the nucleon, and the  $\Delta(1236)$ . The coupling constants and  $\Delta$  propagator are fitted to the appropriate part of the elastic amplitude (the  $P_{33}$  phase shift in the case of Ref. 2). Electromagnetic interactions are introduced with minimal coupling, and gauge invariance is then imposed. The disagreement at low energy between the two types

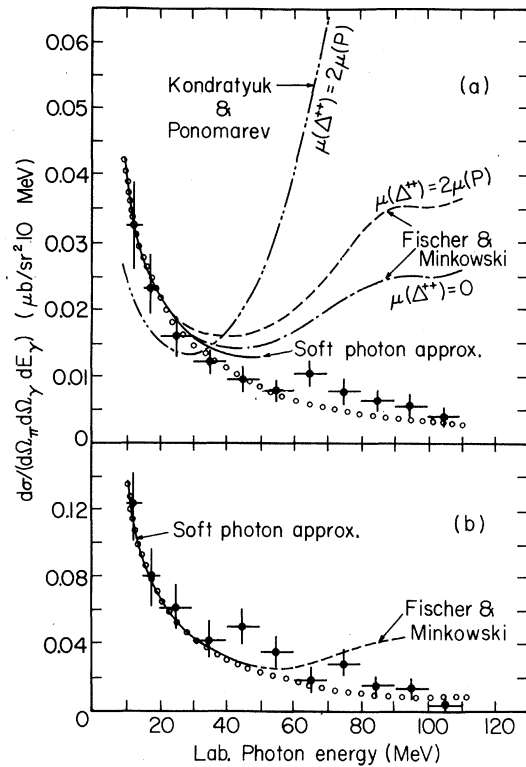


FIG. 3. (a) Experimental cross sections in lab for  $\pi^+p \rightarrow \pi^+p\gamma$  at  $T_\pi = 294$  MeV for geometry in Fig. 2. Errors shown are statistical only. The curves show theoretical calculations adapted to our geometry, based on Refs. 1 and 2. The curve labeled "soft photon approx." is calculated according to Ref. 20. The open circles curve is the equation  $d\sigma/d\hat{\Omega}_\pi d\hat{\Omega}_\gamma dE_\gamma = \sigma_0/(\hat{E}_\gamma)$ . (b) Same as in (a) for  $\pi^-p \rightarrow \pi^-p\gamma$ .

of theory is due to the neglect of the  $S_{31}$  and  $P_{31}$  phase shifts by Ref. 2. In these calculations, we used as our parametrization of the elastic pion-proton scattering amplitudes the Kirsopp CERN I phase shift solution.<sup>18</sup>

We have also briefly investigated the reaction



under the same conditions as Reaction (1) and obtained 110 events. In this process, the interference between the external bremsstrahlung from the pion and proton is constructive, in contrast to the destructive interference in Reaction (1), leading to a large enhancement in the external bremsstrahlung. Furthermore, the dominant intermediate state in Reaction (2) is the  $\Delta^0$  rather than the  $\Delta^{++}$ , and SU(6) predicts that  $\mu(\Delta^0) = 0$ . Our results [Fig. 3(b)] agree with a calculation based on Ref. 1 at low photon energies, but at higher energies show a disagreement similar to

that found in the  $\pi^+p \rightarrow \pi^+p\gamma$  data.

The disagreement of the data with the theoretical predictions is striking. In all the calculations, the presence of the  $\Delta$  resonance is manifested by an increase of the differential cross section with photon energy. (The soft-photon approximation<sup>17</sup> can only be applied up to about 50 MeV in our geometry, since the resonance behavior of the elastic amplitudes violates the conditions of the approximation above this energy.) In contrast, the measured differential cross section falls smoothly and continuously with photon energy.

It should be noted that both measured cross sections agree surprisingly well (see the open-circles curves in Fig. 3), over the entire range of photon energy up to  $\tilde{E}_\gamma = 140$  MeV, with the simple equation

$$d\sigma/d\tilde{\Omega}_\pi d\tilde{\Omega}_\gamma d\tilde{E}_\gamma = \sigma_0/\tilde{E}_\gamma; \quad (3)$$

the tilde denotes a center-of-mass variable, and  $\sigma_0$  is the coefficient of the leading term in the soft-photon approximation in the limit as  $E_\gamma \rightarrow 0$ . This coefficient is calculated from the on-mass-shell elastic scattering amplitude. This simple behavior in the presence of a large resonance is an unexpected feature, which should be examined at other energies and kinematic conditions.

We gratefully acknowledge the hospitality extended to us at the Lawrence Berkeley Laboratory and the skillful help of Mr. Jimmy Vale and crew of the 184 in. cyclotron. It is a pleasure to thank Dr. Ed Dally and the staff of the linear accelerator of the Monterey Naval Postgraduate School for their help in the calibration of the photon detector. We thank Mr. Ray Belisle, Mr. Chris May, and Mr. Gary Segal for assistance in the assembly of the apparatus, and Mr. Martin Thimel for his contributions to the computer pro-

gramming.

\*Work supported in part by the U. S. Atomic Energy Commission.

<sup>1</sup>W. E. Fischer and P. Minkowski, Nucl. Phys. **B36**, 519 (1972).

<sup>2</sup>L. A. Kondratyuk and L. A. Ponomarev, Yad. Fiz. **7**, 111 (1968) [Sov. J. Nucl. Phys. **7**, 82 (1968)].

<sup>3</sup>V. L. Zakharov, L. A. Kondratyuk, and L. A. Ponomarev, Yad. Fiz. **8**, 783 (1968) [Sov. J. Nucl. Phys. **8**, 456 (1969)].

<sup>4</sup>R. Baier *et al.*, Nucl. Phys. **B27**, 589 (1971).

<sup>5</sup>S. C. Bhargava, Nuovo Cimento **58**, 815 (1968).

<sup>6</sup>P. Carruthers and H. W. Huang, Phys. Lett. **24B**, 464 (1967).

<sup>7</sup>P. Carruthers, Phys. Rev. **134**, B638 (1964).

<sup>8</sup>R. E. Cutkosky, Phys. Rev. **109**, 209 (1958), and **113**, 727 (1959).

<sup>9</sup>V. E. Barnes *et al.*, CERN Report No. 63-27 (unpublished).

<sup>10</sup>J. Debaisieux *et al.*, Nucl. Phys. **63**, 273 (1965).

<sup>11</sup>The possible use of photon emission for studying electromagnetic and other properties has been discussed by the following: D. R. Yennie and H. Feshbach, in *Proceedings of the International Conference on High Energy Physics, CERN, 1962*, edited by J. Prentki (CERN Scientific Information Service, Geneva, Switzerland, 1962), p. 219; H. Feshbach and D. R. Yennie, Nucl. Phys. **37**, 150 (1962); S. Barshay and T. Yao, Phys. Rev. **171**, 1708 (1968); S. Barshay and R. Behrends, Phys. Rev. **114**, 931 (1959).

<sup>12</sup>B. T. Feld, *Models of Elementary Particles* (Blaisdell, Waltham, Mass., 1969).

<sup>13</sup>D. Sober, University of California at Los Angeles, Physics Dept. Internal Note No. GN 72-2, 1972 (unpublished).

<sup>14</sup>M. Arman, Ph.D. thesis, University of California at Los Angeles, 1972 (unpublished).

<sup>15</sup>S. Almedeh and C. Lovelace, Nucl. Phys. **B40**, 157 (1972).

<sup>16</sup>B. Barish *et al.*, Phys. Rev. **135**, B416 (1964).

<sup>17</sup>F. E. Low, Phys. Rev. **110**, 974 (1958).

<sup>18</sup>University of California Radiation Laboratory Report No. UCRL-20030  $\pi$ -N Compilation, 1970 (unpublished).